Complete Sequential ^1H and ^{15}N Nuclear Magnetic Resonance Assignments and Solution Secondary Structure of the Blue Copper Protein Azurin from *Pseudomonas aeruginosa*

Mart van de Kamp,[‡,§] Gerard W. Canters,*[,‡] Sybren S. Wijmenga,[§] Arjen Lommen,[‡,§,∥] Cees W. Hilbers,[§] Herbert Nar,[⊥] Albrecht Messerschmidt,[⊥] and Robert Huber[⊥]

Department of Chemistry, Gorlaeus Laboratories, Leiden University, The Netherlands, Laboratory of Biophysical Chemistry, Nijmegen SON Research Center, University of Nijmegen, The Netherlands, and Max Planck Institut für Biochemie, Abteilung Strukturforschung, Martinsried bei München, Germany

Received March 17, 1992; Revised Manuscript Received July 17, 1992

ABSTRACT: Complete sequential ^1H and ^{15}N resonance assignments for the reduced Cu(I) form of the blue copper protein azurin (M_r 14 000, 128 residues) from *Pseudomonas aeruginosa* have been obtained at pH 5.5 and 40 °C by using homo- and heteronuclear two-dimensional (2D) and three-dimensional (3D) nuclear magnetic resonance spectroscopic experiments. Combined analysis of a 3D homonuclear ^1H Hartmann–Hahn nuclear Overhauser (3D ^1H HOHAHA-NOESY) spectrum and a 3D heteronuclear ^1H nuclear Overhauser $^1H\{^{15}N\}$ single-quantum coherence (3D $^1H\{^{15}N\}$ NOESY-HSQC) spectrum proved especially useful. The latter spectrum was recorded without irradiation of the water signal and provided for differential main chain amide (NH) exchange rates. NMR data were used to determine the secondary structure of azurin in solution. Comparison with the secondary structure of azurin obtained from X-ray analysis shows a virtually complete resemblance; the two β-sheets and a 3_{10}–α–3_{10} helix are preserved at 40 °C, and most loops contain well-defined turns. Special findings are the unexpectedly slow exchange of the Asn-47 and Phe-114 NH's and the observation of His-46 and His-117 $N^{\epsilon 2}H$ resonances. The implications of these observations for the assignment of azurin resonance Raman spectra, the rigidity of the blue copper site, and the electron transfer mechanism of azurin are discussed.

The small and soluble Cu-containing protein azurin (128 amino acid residues; M_r 14K) from *Pseudomonas aeruginosa* fulfills a role in electron transfer in the periplasm of this bacterium when it grows under denitrifying conditions (Parr et al., 1976; Henry & Bessières, 1984). As a first step to probe its structure in solution, and to facilitate the study of its dynamics as related to its function, we report here the nearly complete ^1H and ^{15}N nuclear magnetic resonance (NMR) assignments of the reduced Cu(I) form of the protein, as they were obtained from the analysis of two- and three-dimensional (2D and 3D)[1] homo- and heteronuclear spectra. Using these assignments, the secondary structure of azurin in solution is established, and a qualitative determination of the rate of exchange of its main chain amide protons is accomplished.

Azurin belongs to the class of type I, so-called blue copper proteins [for reviews, see e.g., Adman (1985, 1991) and Sykes (1991)]. Other members of this class of proteins are, e.g., the plastocyanins, amicyanins, stellacyanins, and pseudo-azurins. The Cu sites of these proteins have a number of characteristics in common, including an intense absorption band at about 600 nm, a small hyperfine splitting constant in the $g_\parallel$ region of their EPR spectra, and a relatively high midpoint potential. The Cu ion in *P. aeruginosa* azurin is coordinated by atoms from four side chains (Cys-112 $S^{\gamma-}$, His-46 and His-117 $N^{\delta 1}$, and Met-121 S^{δ}) and the oxygen of the main chain carbonyl group of Gly-45 (Nar et al., 1991a,b).

Because of their small size and high stability, blue copper proteins are well suited for study by NMR spectroscopy. So far, this has resulted in complete sequential assignments for three plastocyanins [from spinach (Driscoll et al., 1987), French bean (Chazin et al., 1988; Chazin & Wright, 1988), and the green alga *Scenedesmus obliquus* (Moore et al., 1988a)] and one amicyanin [from *Thiobacillus versutus* (Lommen et al., 1991)]. These assignments have enabled the calculation of the solution structures of the plastocyanins from *S. obliquus* (Moore et al., 1988b) and French bean (Moore et al., 1991) and the *T. versutus* amicyanin (Kalverda et al., 1991).

Although *P. aeruginosa* azurin has been the subject of various NMR experiments over the last years (Hill et al., 1976a,b; Ugurbil et al., 1977; Ugurbil & Bersohn, 1977; Hill & Smith, 1979; Adman et al., 1982; Blaszak et al., 1982; Canters et al., 1984a,b; Ugurbil & Mitra, 1985; Groeneveld et al., 1985, 1988; Van de Kamp et al., 1990a,b,c) none of these has provided complete sequential assignments. These are considered to be opportune in view of the questions generated by recent site-directed mutagenesis studies. By employing various azurin mutants, it was demonstrated that a surface region with a high content of apolar amino acids, the so-called hydrophobic patch, mediates electron transfer

* To whom correspondence should be addressed.
‡ Leiden University.
§ University of Nijmegen.
∥ Present address: RIKILT, Wageningen, The Netherlands.
⊥ Max Planck Institut für Biochemie, Martinsried.

[1] Abbreviations: 1-, 2-, and 3D, one, two, and three dimensional; COSY, correlation spectroscopy; δ, chemical shift; DQF-COSY, double-quantum filtered COSY; DSS, 4,4-dimethyl-4-silapentane-1-sulfonate; $d_{XY}(i,i+1)$, NOE between proton X on residue i and proton Y on residue $i+1$; H-bond, hydrogen bond; HM(/S)QC, heteronuclear multiple (/single) quantum coherence; HOHAHA, homonuclear Hartmann–Hahn; INEPT, insensitive nuclei enhanced by polarization transfer; IPTG, isopropyl β-D-thiogalactopyranoside; M_r, relative molecular mass; NOE, nuclear Overhauser effect; NOESY, NOE spectroscopy; RR, resonance Raman; SCUBA, stimulated cross-peaks under bleached alphas; TMA, tetramethylammonium nitrate; TPPI, time-proportional phase incrementation; wt, wild type.

0006-2960/92/0431-10194$03.00/0

between azurin and its purported physiological redox partners, nitrite reductase and cytochrome c_{551} (Van de Kamp et al., 1990b). It is important to know the dynamic properties of this surface, since these may be expected to affect the specificity and rate of electron transfer. Secondly, some azurin mutants show differences in spectroscopic properties relative to the wild-type (wt) protein that might be due to structural changes (Van de Kamp et al., 1990a,b). Although structures of some mutant azurins have been obtained by X-ray crystallography (Nar et al., 1991a), not all mutant azurins appear easily crystallizable. Moreover, solution structures may differ from crystal structures. The determination of the solution structure of azurin is therefore important. Finally, the purported inflexibility of the Cu site (Nar et al., 1991a,b), the kinetics of the protonation of His-35 (Hill & Smith, 1979; Nar et al., 1991b), and the solvation of azurin are all topics that can be addressed by NMR studies. A prerequisite for this is the complete resonance assignment of the wt azurin NMR spectrum, which is reported here.

EXPERIMENTAL PROCEDURES

Isolation and ^{15}N Labeling of Azurin. Unlabeled azurin was isolated from *Escherichia coli* KMBL1164 cells that were transformed with plasmid pGC5 which contains the *P. aeruginosa* azurin encoding *azu* gene, as described previously (Van de Kamp et al., 1990c). Uniformly ^{15}N-labeled azurin was isolated from pGC5 harboring *E. coli* MH1 cells (Goddard et al., 1983) grown on minimal medium with 0.5 g/L $^{15}NH_4Cl$ (Muchmore et al., 1989), 1 mL/L of a trace element solution (Light & Garland, 1971), ampicillin and streptomycin (Sambrook et al., 1989), and additonal copper (final concentration 10 μM $CuSO_4$). When the optical density of the growing culture was 1.0, expression of the *azu* gene was induced by the addition of IPTG to a final concentration of 0.2 mM. After continuation of growth for 3 h, cells were harvested and uniformly labeled [^{15}N]azurin was isolated using the same purification method as for unlabeled azurin. ^{15}N incorporation was checked by 1D ^{15}N INEPT NMR spectroscopy.

NMR Sample Preparation. NMR samples of reduced [Cu(I)]azurin were prepared as described previously (Van de Kamp et al., 1990b,c). The sample buffer was 25 mM potassium phosphate (pH 5.5) either in 90% H_2O/10% D_2O or in 99.95% D_2O. A partially oxidized sample in H_2O was prepared by adding up to 10% of oxidized [Cu(II)] azurin in 25 mM potassium phosphate (pH 5.5) to a fully reduced azurin sample. H/D exchange in the D_2O sample was promoted by keeping the sample for several hours at pH 8.5 and 40 °C before measurement.

NMR samples contained 3–6 mM unlabeled azurin or 1.5–2.5 mM ^{15}N-labeled azurin. Sample volumes were 450–500 μL. Under the chosen experimental conditions (pH 5.5, 40 °C), reduced and oxidized azurin exist as stable monomers in solution, and reduced azurin does not oxidize for periods of up to a week.

In addition, two 2 mM samples were prepared, containing fully oxidized or reduced unlabeled azurin that was dissolved in 0.1 M formate buffer (pH 7.0) in 99.95% D_2O by using ultrafiltration at 5 °C, which took 4 h. These samples were used only for 1D ^1H NMR experiments.

NMR Spectroscopy. 1D ^1H NMR spectra, recorded to follow long-term NH exchange at pH 7, were acquired on a 300-MHz Bruker WM300 spectrometer. Samples of either Cu(I) or Cu(II) azurin were directly placed in the spectrometer after uptake in formate buffer in D_2O (see above), and measurement of 1D ^1H NMR spectra at 37 °C was immediately started after a 30-min interval, needed for adjustment of spectrometer parameters. Subsequently, one spectrum was obtained every 30 min over a period of 16 h. About 800 transients were accumulated per FID in 16K memory space for one spectrum. Spectral width was 4000 Hz.

1D ^1H-decoupled ^{15}N INEPT NMR spectra (Morris & Freeman, 1979) were measured as a function of temperature (10, 20, 30, and 40 °C) at 40.56 MHz on a Bruker MSL400 spectrometer equipped with a broad-band probe. The delay time $1/(4 \times {}^1J_{NH})$ was set to 2.75 ms. The relaxation delay was set to 1.2 s. The ^{15}N spectral width was set to 10 000 Hz centered around the carrier position at 112 ppm relative to liquid ammonia. A total of 2000 transients were acquired per FID in 16K memory space.

All 2D and 3D NMR spectra were recorded on a 600-MHz Bruker AM600 spectrometer. A normal, selective ^1H probe was used for homonuclear ^1H measurements, and an inverse probe was used for heteronuclear $^1H\{^{15}N\}$ measurements. ^{15}N-decoupling was achieved with a continuous broad-band amplifying facility (Bruker BFX-5) by using the GARP (Shaka et al., 1985) composite pulse decoupling sequence. During the 3D experiments an AM timer box was used to reduce I/O time (Kay et al., 1989).

The different 2D and 3D NMR experiments that were used to study reduced azurin are collected in Table I. Reduction of the ^{15}N spectral width in some 2D and 3D $^1H\{^{15}N\}$ spectra from 10 to 3 kHz resulted in folding of His and Arg side-chain resonances into otherwise empty regions of the spectrum. Reduction of the F_1 ^1H spectral width from 10 to 5 kHz in one of the 3D $^1H\{^{15}N\}$ NOESY-HSQC spectra also resulted in folding but caused some overlap too. Both reductions increased the spectral resolution. In the 3D $^1H\{^{15}N\}$ NOESY-HSQC experiment with a F_1 ^1H spectral width of 10 kHz, a trim pulse was applied to destroy the water magnetization by randomization (Messerle et al., 1989) instead of using phase-locked presaturation of the water signal.

Data Processing. 1D NMR spectra were processed on a Bruker Aspect 2000 computer using standard routines. 2D NMR data processing was performed on a Bruker X32 workstation using standard Bruker NMR software. 3D NMR data were processed on a SUN Sparc workstation using the NMRi 2D software program NMR2 (New Methods Research Inc., Syracuse, NY) in combination with some routines which were either made available by Drs. A. Bax and L. E. Kay or in-house-written. Routinely, the data were zero-filled once in each dimension, multiplied with a $\pi/2$ (especially used for the F_1 and/or F_2 dimensions of the 3D spectra), $\pi/3$, $\pi/4$, or $\pi/5$ shifted squared sine-bell apodization function, Fourier transformed, interactively phase corrected, and baseline corrected. The data in the F_1 NOESY dimension of the 3D $^1H\{^{15}N\}$ NOESY-HSQC spectrum, which was recorded without water presaturation, were zero-filled three times (from 256 to 2048 complex points) instead of once. Final digital resolutions are summarized in Table I.

^1H and ^{15}N calibration was performed by recording 1D spectra on a sample with TMA and with $(^{15}NH_4)_2SO_4$. Quoted ^1H chemical shifts are referenced to DSS, and ^{15}N chemical shifts are relative to liquid ammonia.

RESULTS

Spin System Assignments. Spectral investigation was started with the analysis of 2D ^1H DQF-COSY and HOHAHA spectra, aimed at the definition of spin systems (Wüthrich, 1986). A total of 118 NH–$C^\alpha H$ cross peaks were

Table I: 2D (A) and 3D (B) NMR Experiments Used To Study Reduced Cu(I) Azurin[a]

(A) 2D Experiments

experiment	solvent	Cu^I/Cu^{II} (%)	mixing time (ms)	spectral width F_1/F_2 (kHz)	NI[b] t_1	NS[c]/FID	resolution[d] F_1/F_2 (ppm/point)	ref[e]
^{1}H DQF-COSY	D_2O	100/0		8.06/8.06	512	32	0.013/0.006	1
	H_2O	100/0		10.00/10.00	512	32	0.016/0.008	
	H_2O[h]	100/0		10.00/10.00	512	32	0.016/0.008	
	H_2O	90/10		10.00/10.00	512	32	0.016/0.008	
^{1}H HOHAHA	D_2O	100/0	35[j]	8.06/8.06	512	32	0.013/0.006	2, 3
	H_2O	100/0	26[j]	10.00/10.00	512	32	0.016/0.008	
	H_2O	100/0	45[j]	10.00/10.00	512	32	0.016/0.008	
^{1}H NOESY	D_2O	100/0	100[k]	8.06/8.06	512	32	0.013/0.006	4, 5
	D_2O	100/0	125[k]	8.06/8.06	512	32	0.013/0.006	
^{1}H SCUBA[f]-NOESY	H_2O	100/0	100[k]	10.00/10.00	512	32	0.016/0.008	
	H_2O	100/0	150[k]	10.00/10.00	512	32	0.016/0.008	
	H_2O	90/10	100[k]	10.00/10.00	512	32	0.016/0.008	
^{1}H{^{15}N} HMQC[g]	H_2O	100/0		10.00/10.00	128	16	0.65/0.008	6, 7
	H_2O	100/0		3.00/10.00	128	16	0.19/0.008	

(B) 3D Experiments

experiment	solvent	Cu^I/Cu^{II} (%)	mixing time (ms)	spectral width $F_1/F_2/F_3$ (kHz)	NI t_1/t_2	NS/FID	resolution $F_1/F_2/F_3$ (ppm/point)	ref
^{1}H HOHAHA-NOESY	H_2O	100/0	35[j]/100[k]	9.26/9.26/9.26	256/128	8	0.06/0.12/0.015	8, 9, 10
^{1}H{^{15}N} NOESY-HSQC[g]	H_2O	100/0	100[k]	5.00/3.00/10.00	256/60[l]	8	0.033/0.77/0.016	11, 12
	H_2O[i]	100/0	100[k]	10.00/3.00/10.00	256/82	8	0.016/0.39/0.016	

[a] Routinely, spectra were recorded at 40 °C on a 600-MHz spectrometer, using low-power phase-locked presaturation of the water signal during the 1.0–1.5-s relaxation delay, and using TPPI for quadrature detection (Marion & Wüthrich, 1983). Data were acquired in 2K memory space in the 2D experiments and in 1K in the 3D experiments. Optimization of the receiver phase was performed to reduce baseline distortions (Marion & Bax, 1988). [b] Number of increments. [c] Number of scans per FID. [d] Final digital resolution after processing. [e] References: (1) Rance et al. (1983); (2) Braunschweiler and Ernst (1983); (3) Bax and Davis (1985); (4) Kumar et al. (1980); (5) Macura et al. (1982); (6) Bax et al. (1983); (7) Bax et al. (1990); (8) Griesinger et al. (1989); (9) Oschkinat et al. (1989); (10) Wijmenga and Van Mierlo (1991); (11) Marion et al. (1989a); (12) Fesik and Zuiderweg (1990). [f] The SCUBA (Brown et al., 1988) delay time was set to 100 ms. [g] The $1/(2 \times {}^1J_{NH})$ delay in the HMQC and HSQC pulse sequences was set to 4.5 ms. The ^{15}N carrier position was placed in the middle of the main-chain amide region at δ = 115 ppm (relative to liquid ammonia). [h] Recorded at 30 °C. [i] Water suppression was achieved by the application of a 2-ms trim pulse (Messerle et al., 1989). [j] Spin-lock time. In the HOHAHA experiments the Clean-MLEV17 sequence (Griesinger et al., 1988) was used for spin-locking. The spin-lock time includes two 2.5-ms trim pulses applied before and after the MLEV17 mixing period. [k] NOE buildup time. [l] Phase cycling in F_2 was done by the method of States et al. (1982).

found in the NH–C$^\alpha$H fingerprint regions of DQF-COSY spectra recorded at 40 °C in H_2O and D_2O (Figure 1A,C) and at 30 °C in H_2O. The maximum number of cross peaks is 134, because azurin (128 residues) has 4 prolines and 11 glycines, and the N-terminal NH is probably exchanging rapidly. Alignment of the amide region of the 45-ms 2D HOHAHA spectrum, which was recorded for an azurin sample in H_2O, with the aliphatic region of the 35-ms HOHAHA spectrum, recorded for a sample in D_2O, provided for 120 spin systems out of 123 detectable ones.

Sequential Assignments. By using 2D NOESY spectra, sequential assignment (Wüthrich, 1986; Englander & Wand, 1987) was readily performed for residues 4–8, 17–24, 29–34, 49–53, 92–97, 106–111, and 122–127. These stretches of residues occur in seven of the eight β-strands that make up the β-sheet structure of the protein (see below). Outside these stretches, sequential assignment was less unequivocal. Therefore, we turned to 3D NMR spectroscopy [for reviews, see, e.g., Griesinger et al. (1989), Fesik and Zuiderweg (1990), and Clore and Gronenborn (1991)]. Our approach involved the combined use of a 3D ^{1}H HOHAHA-NOESY spectrum and a 3D ^{1}H{^{15}N} NOESY-HSQC spectrum.

Sequential assignments were obtained from a 3D ^{1}H HOHAHA-NOESY spectrum by using F_1F_3 and F_1F_2 planes, according to the approach introduced by Wijmenga and Van Mierlo (1991). It was shown there that, in an F_1F_3 plane drawn through a particular resonance at ω_2, e.g., ω_2 = C$^\alpha$H$_i$, the spin-lock connectivity pattern of residue i through the C$^\alpha$H$_i$ resonance is repeated parallel to F_1 at all resonance positions along F_3 at which NOEs with C$^\alpha$H$_i$ are present. The proton resonances that have NOE connectivities with the C$^\alpha$H$_i$ resonance are thus identified. At this point no unambiguous discrimination is possible between intra- and interresidue NOEs. Such a discrimination and subsequent assignment is feasible by using the corresponding F_1F_2 plane through ω_3 = C$^\alpha$H$_i$. At the F_2 positions of the NOE connectivities with C$^\alpha$H$_i$ (that are on the diagonal now), the spin-lock pattern of residue i (which was present at the F_3 positions of the NOEs in the F_1F_3 plane) is replaced by the own spin-lock patterns of the protons to which NOEs are observed. Assignments can be checked by using the F_1F_3 and F_1F_2 planes through the ω_2 and the ω_3 resonance positions of these protons that have NOE contacts with C$^\alpha$H$_i$. These principles are illustrated in Figure 2 for F_1F_3 and F_1F_2 planes through the C$^\alpha$H resonances of Asp-6 and Thr-96.

Analysis of the 3D ^{1}H HOHAHA-NOESY spectrum provided for full sequential assignments, including assignments for the four proline residues. These assignments were confirmed by analysis of the 3D ^{1}H{^{15}N} NOESY-HSQC spectra. This analysis was performed according to the procedure described by Driscoll et al. (1990), using F_1F_3 ^{1}H/^{1}H slices through ω_2 = ^{15}N of the respective residues. Figure 3 shows such F_1F_3 slices for residues Cys-112 to Lys-128, taken from the 3D ^{1}H{^{15}N} NOESY-HSQC spectrum that was recorded without presaturation of the water signal. This region comprises the Cu ligand loop (copper ligands being Cys-112, His-117, and Met-121) and the eight C-terminal residues of azurin that form a β-strand (see below).

A 3D ^{1}H{^{15}N} NOESY-HSQC spectrum does not contain information which allows discrimination between intra- and

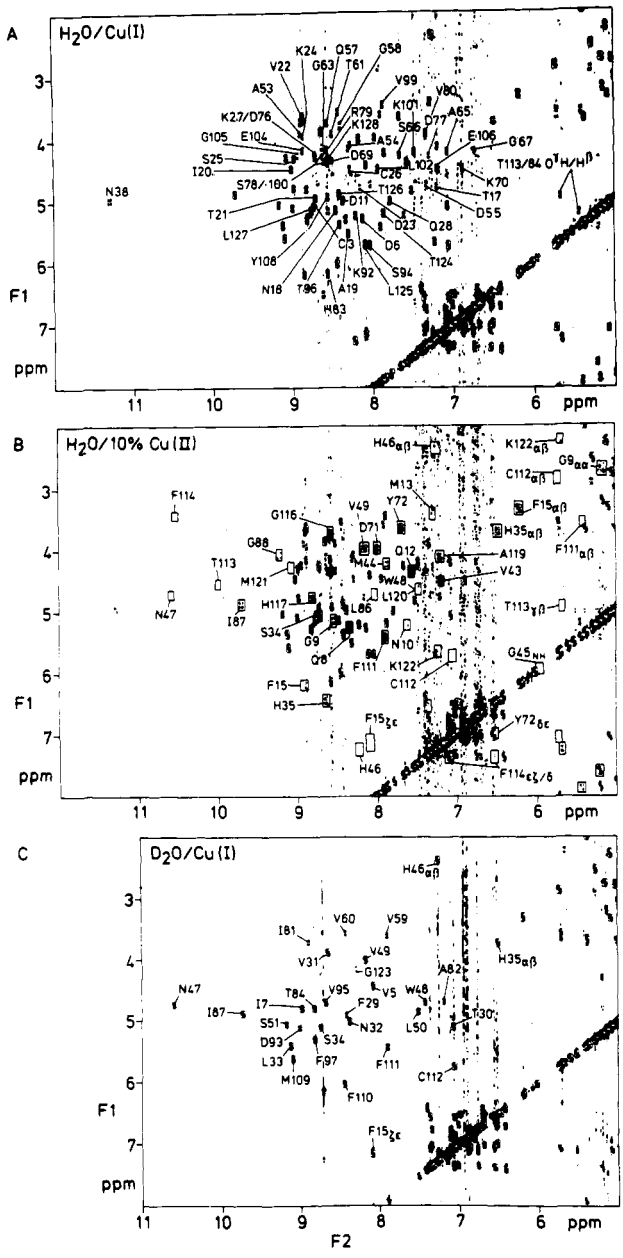

FIGURE 1: NH–C$^{\alpha}$H regions of 2D DQF-COSY spectra (recorded at 40 °C) of (A) fully reduced Cu(I) azurin in 90% H_2O/10% D_2O, (B) partially oxidized [10% Cu(II)] azurin in 90% H_2O/10% D_2O, and (C) fully reduced Cu(I) azurin in 99.95% D_2O. Peaks that are broadened in spectrum B are boxed, and their assignments are indicated. Assignments that are given in spectra B and C are not given in spectrum A. In addition, some aliphatic, aromatic, and C$^{\beta}$H–O$^{\gamma 1}$H cross-peak assignments are indicated. Some NH–C$^{\alpha}$H cross peaks are present below the lowest contour level in panel A (residues 41, 47, 52, 68, 73, 85, 88, 95, 98, 107, 113, and 114) and in panel C (residues 46, 72, 73, 113, and 114). Some NH–C$^{\alpha}$H cross peaks, which are not or hardly visible at 40 °C, because they nearly coincide with the water signal, are better visible at 30 °C (residues 2, 4, 14, 16, 48, 91, 103, and 120).

interresidue NOEs. Usually, intraresidue NOEs in a 3D ^{1}H-{^{15}N} NOESY-HSQC spectrum are identified and assigned by alignment with a 3D ^{1}H{^{15}N} HOHAHA-HSQC spectrum (Marion et al., 1989b; Driscoll et al., 1990). However, this assignment can be ambiguous (a) when there is overlap in the F_1 dimension or (b) when HOHAHA transfer in the HOHAHA-HSQC experiment is inefficient. Those problems can be overcome by using a 3D ^{1}H HOHAHA-NOESY spectrum to assign the NOE cross peaks in a 3D ^{1}H{^{15}N} NOESY-HSQC spectrum as illustrated in Figure 4 for Trp-48 and Ile-81. The alignment of the 3D ^{1}H{^{15}N} NOESY-HSQC spectrum with the 3D ^{1}H HOHAHA-NOESY spectrum thus enabled us to obtain a virtually complete and unambiguous assignment of all cross peaks in the 3D ^{1}H{^{15}N} spectrum.

The sequential assignments are collected in Table II. Their reliability is reflected in Figure 5 by the presence of continuous $d_{\alpha N}(i,i+1)$ NOEs [$d_{\alpha\delta}(i,i+1)$ for $i+1$ being a Pro], nearly continuous $d_{\beta N}(i,i+1)$ NOEs, various stretches of $d_{NN}(i,i+1)$ NOEs, and large numbers of medium-range NOEs. In summary, by using 3D spectra, the sequential assignment could be performed in an unambiguous way for the whole protein.

Side-Chain Assignments. Side-chain assignments were obtained by using 2D COSY, HOHAHA, and NOESY spectra, both in H_2O and D_2O, and by using HOHAHA information present in the 3D ^{1}H HOHAHA-NOESY spectrum and sequential ($i,i-1$) NOE connectivities in the 3D ^{1}H{^{15}} NOESY-HSQC spectrum. Distinction between C$^{\beta}$H, C$^{\gamma}$H, and C$^{\delta}$H resonances was made by using the 2D DQF-COSY spectrum recorded in D_2O. When difficulties arose due to overlap, additional use was made of HOHAHA information.

Resonances could be assigned to the following exchangeable side-chain protons: all Asn N$^{\gamma}$H$_2$s and Gln N$^{\delta}$H$_2$s, His-46 and His-117 N$^{\epsilon 2}$H, Trp-48 N$^{\epsilon 1}$H, Arg-79 N$^{\epsilon}$H and N$^{\eta}$H, and Thr-84 and Thr-113 O$^{\gamma 1}$H. The detection of Lys N$^{\zeta}$H resonances was prohibited by their high exchange rate at 40 °C, as became evident from investigation of the temperature dependence of the 1D ^{15}N INEPT spectrum of azurin (data not shown). Met C$^{\epsilon}$H$_3$ resonances were identified from the observation of $d_{\epsilon\gamma}$ and $d_{\epsilon\beta}(i,i)$ NOEs. Of all Phe and Tyr residues, only the Phe-110 ring is slowly flipping at 40 °C, which enabled the observation of five well-defined aromatic resonances.

Eventually, complete ^{15}N and ^{1}H resonance assignments were obtained for 121 residues, and partial assignments were obtained for 7 (mostly long side chain) residues. These assignments are collected in Table II.

Secondary Structure. The recognition and definition of secondary structure elements was based upon NOEs and $^3J_{HN\alpha}$ values [see Wüthrich (1986) and references therein]. Large line widths made it impossible to obtain accurate $^3J_{HN\alpha}$ values from analysis of DQF-COSY NH–C$^{\alpha}$H cross peaks. $^3J_{HN\alpha}$ values were therefore obtained from the analysis of NH–C$^{\alpha}$H cross peak intensities in the 26-ms 2D Clean-HOHAHA spectrum. Numerical simulation has shown that when short spin-lock times (i.e., ≤30 ms) are used, as is the case here, these intensities are proportional to $(^3J_{HN\alpha})^2$ (Cavanagh et al., 1990; Oschkinat et al., 1990). The precision of the $^3J_{HN\alpha}$ values is 1–1.5 Hz. This takes into account relaxation and off-resonance effects (Bax, 1989) and the effects of side-chain coupling constants (Cavanagh et al., 1990) on the intensity of the NH–C$^{\alpha}$H cross peak. NOE effects upon the HOHAHA cross-peak intensities were eliminated by using the Clean-MLEV17 pulse sequence for spin-locking (Griesinger et al., 1988). In our case, only two broad classes of $^3J_{HN\alpha}$ couplings were distinguished: couplings smaller than 6 Hz and couplings larger than 8 Hz.

Main-chain H-bonds are indicated in the secondary structure (Figure 6) when they are an established part of regular secondary structure elements like parallel and antiparallel β-sheet, α-helix, and tight and helical turns.

The secondary structure of azurin as derived from the NMR data contains two β-sheets, a helix, and 12 tight and 4 helical turns (Figure 6). They are briefly discussed hereafter.

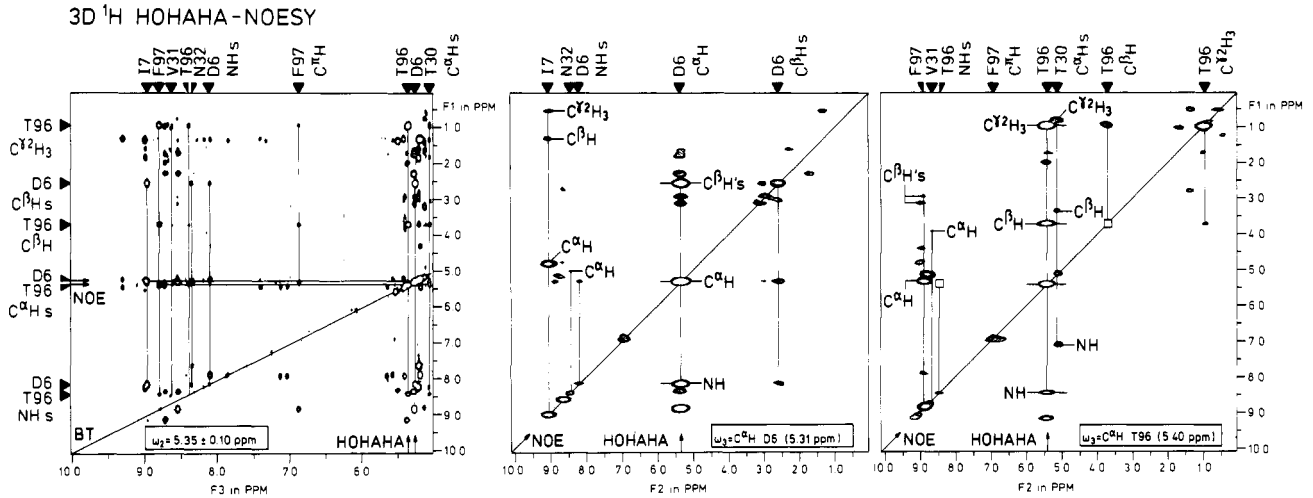

FIGURE 2: F_1F_3 plane (at ω_2 of both Asp-6 and Thr-96 C$^\alpha$Hs) and two F_1F_2 planes [at ω_3 of Asp-6 and Thr-96 C$^\alpha$H (see insert)] from the 3D ^{1}H Clean HOHAHA-NOESY spectrum of Cu(I) azurin in 90% H_2O/10% D_2O. (Note that although the C$^\alpha$H resonances of Asp-6 and Thr-96 have slightly different chemical shifts, they are observed in the same F_1F_3 plane because of the limited resolution in the F_2 dimension.) NOEs with Asp-6 or Thr-96 C$^\alpha$H are identified in the F_1F_3 plane through both C$^\alpha$Hs by the observation that either the Asp-6 or Thr-96 C$^\alpha$H spin-lock pattern (parallel to F_1) is repeated on them. These NOEs are assigned by using the F_1F_2 planes through Asp-6 C$^\alpha$H and Thr-96 C$^\alpha$H, where they have their own spin-lock patterns. As Asp-6 is present in a parallel β-sheet structure and Thr-96 is located in an antiparallel β-sheet structure (Figure 6), long-range NOEs typical for these structures are visible, alongside with strong sequential $d_{\alpha N}(i,i+1)$ and intraresidual $d_{\alpha N}(i,i)$, $d_{\alpha\beta}(i,i)$, and $d_{\alpha\gamma}(i,i)$ NOEs.

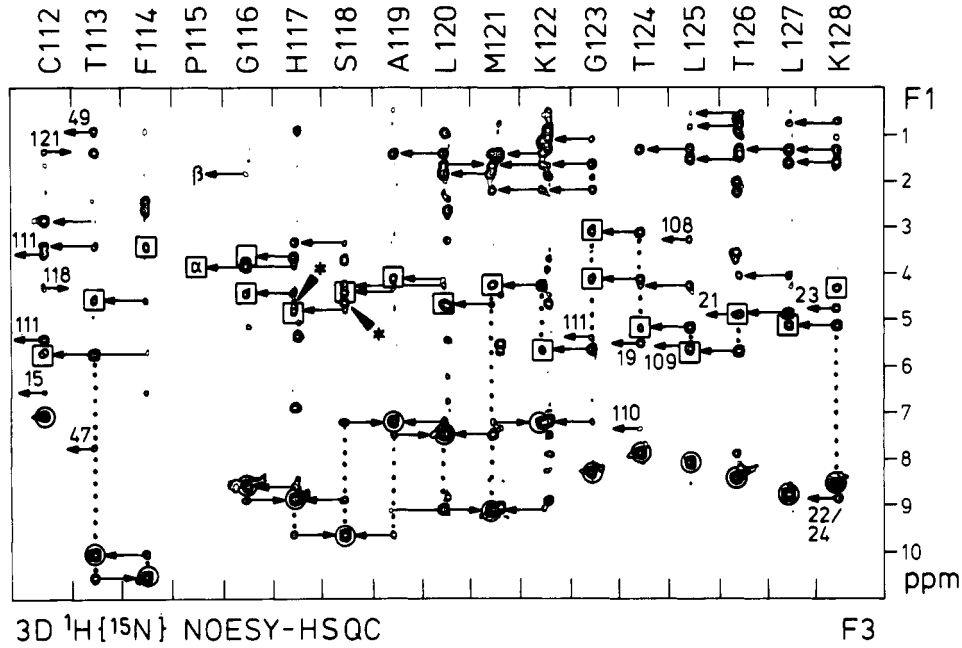

FIGURE 3: F_1F_3 ^{1}H/^{1}H slices containing ^{15}NH-NOESY lines from the 3D ^{1}H{^{15}N} NOESY-HSQC spectrum recorded without water presaturation, at the respective ω_2 positions of the ^{15}N chemical shifts of residues Cys-112–Lys-128. The main-chain ^{15}NH HSQC peaks are circled, and intraresidue $d_{N\alpha}(i,i)$ connectivities are boxed. The C$^\alpha$H and C$^\beta$H resonance positions of Pro-115 are indicated for convenience. Short- and medium-range NOEs are indicated by arrows, while long-range NOEs have their arrows numbered by the residue wherewith NOE transfer occurs. Interresidue NOEs are between the NH of the residue from which the arrows start and the proton to which the resonance at which the arrows point is assigned [thus the strong sequential $d_{N\alpha}(i,i-1)$ NOEs in the last seven F_1F_3 slices point at the boxed, generally weaker intraresidue $d_{N\alpha}(i-1,i-1)$ NOEs]. The principal sequential pathway, via $d_{N\alpha}(i,i-1)$ NOEs for residues 112–113 and 121–128 and via $d_{NN}(i,i-1)$ NOEs for residues 113–114 and 116–121, is indicated by the dotted lines. The ^{15}NH-NOESY lines of Leu-120, Met-121, Lys-122, and Thr-126 slightly overlap with the ^{15}NH lines of other residues. Large arrowheads, marked with an asterisk, denote ^{15}NH–H_2O exchange cross peaks present on the waterline. Note the absence of NH exchange peaks for residues Cys-112–Phe-114 (in the first part of the Cu ligand loop) and residues Met-121 to Lys-128 (that form β-strand S8). The ^{15}NH–H_2O cross peaks of residues 119 and 120 are below the plot level.

(*a*) *β-Sheets.* Azurin in solution consists of two β-sheets, comprising eight β-strands, numbered S1 to S8. Numbering of the strands is according to Nar et al. (1991a). The high density of interstrand NOEs shows that each β-sheet is tightly packed. This is confirmed by the observation of very slow exchange (on the time scale of hours to days) of the NHs that are involved in the H-bonds between the β-strands (see below and Figure 5). The two β-sheets are connected by two loops at the "southern" end and two loops at the "northern" end of the molecule and by a short loop between strands S2a and S2b. No main chain to main chain NOEs are observed between β-strands S5 and S6, but some main chain to side chain NOEs are present, namely, between Lys-85 NH and Asp-93 C$^\beta$H, between Gly-88 NH and Glu-91 C$^\beta$H, and between Val-95 NH and Thr-84 C$^{\gamma 2}$H$_3$. A bulging structure interrupts β-strand S5 at the position of Lys-85 and Leu-86; these residues are opposed by only one amino acid, Asn-47, in strand S4. The presence of this bulging structure is inferred

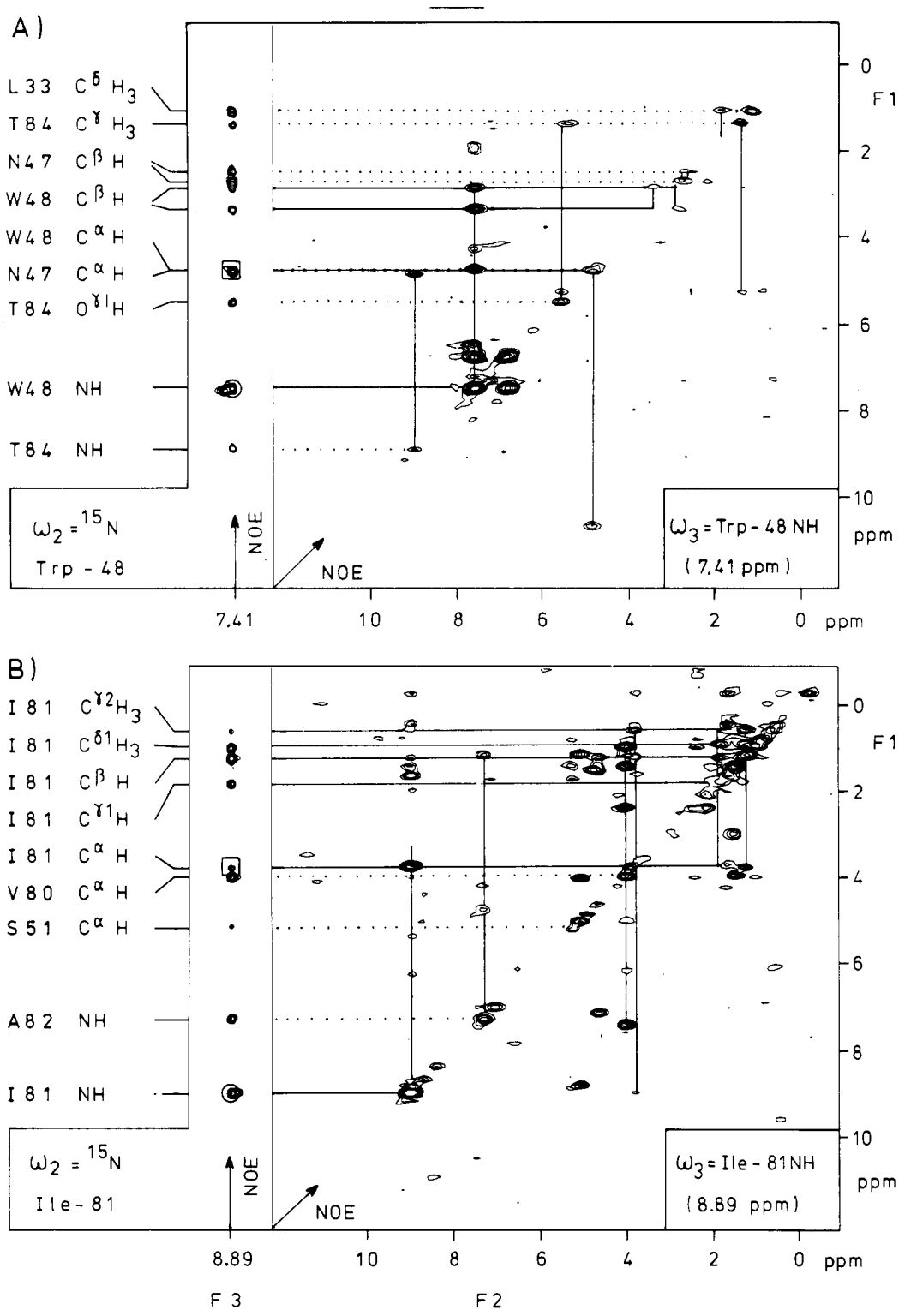

FIGURE 4: Illustration of the use of F_1F_2 planes from a 3D ^{1}H HOHAHA-NOESY spectrum to discriminate between, and to assign intra- and interresidue NOEs on, a ^{15}NH-NOESY line located on a F_1F_3 slice from a 3D ^{1}H{^{15}N} NOESY-HSQC spectrum for two cases in which such a discrimination and subsequent assignment would not be feasible by the comparison of F_1F_3 slices from 3D ^{1}H{^{15}N} HOHAHA- and NOESY-HSQC spectra. NOE assignments are indicated along the F_1 axis. On the ^{15}NH-NOESY lines, the main-chain ^{15}NH HSQC peaks are circled, and intraresidue $d_{N\alpha}(i,i)$ connectivities are boxed. The lines in the F_1F_2 plane that are parallel with F_1 represent spin-lock patterns, which facilitate the NOE assignments. Intraresidue and interresidue NOEs on the ^{15}NH-NOESY line are connectd to the corresponding spin-lock patterns via solid (—) and dotted (···) horizontal lines, respectively. (A) Trp-48 ^{15}NH-NOESY line with F_1F_2 plane through Trp-48 NH. On the Trp-48 ^{15}NH NOESY line, a strong NOE cross peak is present at 4.7 ppm. Since the C$^\alpha$Hs of Trp-48 and Asn-47 both resonate at about 4.7 ppm, it would not be possible to establish from the combined use of 3D ^{1}H{^{15}N} NOESY- and HOHAHA-HSQC spectra whether the cross peak at 4.7 ppm represents an intra- or an interresidue NOE. However, the F_1F_2 plane shows that it consists of a strong interresidue NOE with Asn-47 C$^\alpha$H with at most a very weak intraresidue NOE with Trp-48 C$^\alpha$H. (B) Ile-81 ^{15}NH-NOESY line with F_1F_2 plane through Ile-81 NH. The F_1F_2 plane shows that spin-lock transfer starting at Ile-81 NH does not go beyond the C$^\alpha$H (the weak high-field cross peaks belong to other spin-lock patterns that have higher intensity in adjacent F_1F_2 planes). Therefore, discrimination between intra- and interresidue NOEs on the high-field part of the Ile-81 ^{15}NH-NOESY line is expected to be not well feasible by comparison with the Ile-81 spin-lock pattern in a 3D ^{1}H{^{15}N} HOHAHA-HSQC spectrum. However, the spin-lock patterns that appear on the NOE connectivities in the F_1F_2 plane facilitate both this discrimination and unambiguous assignment of these NOEs.

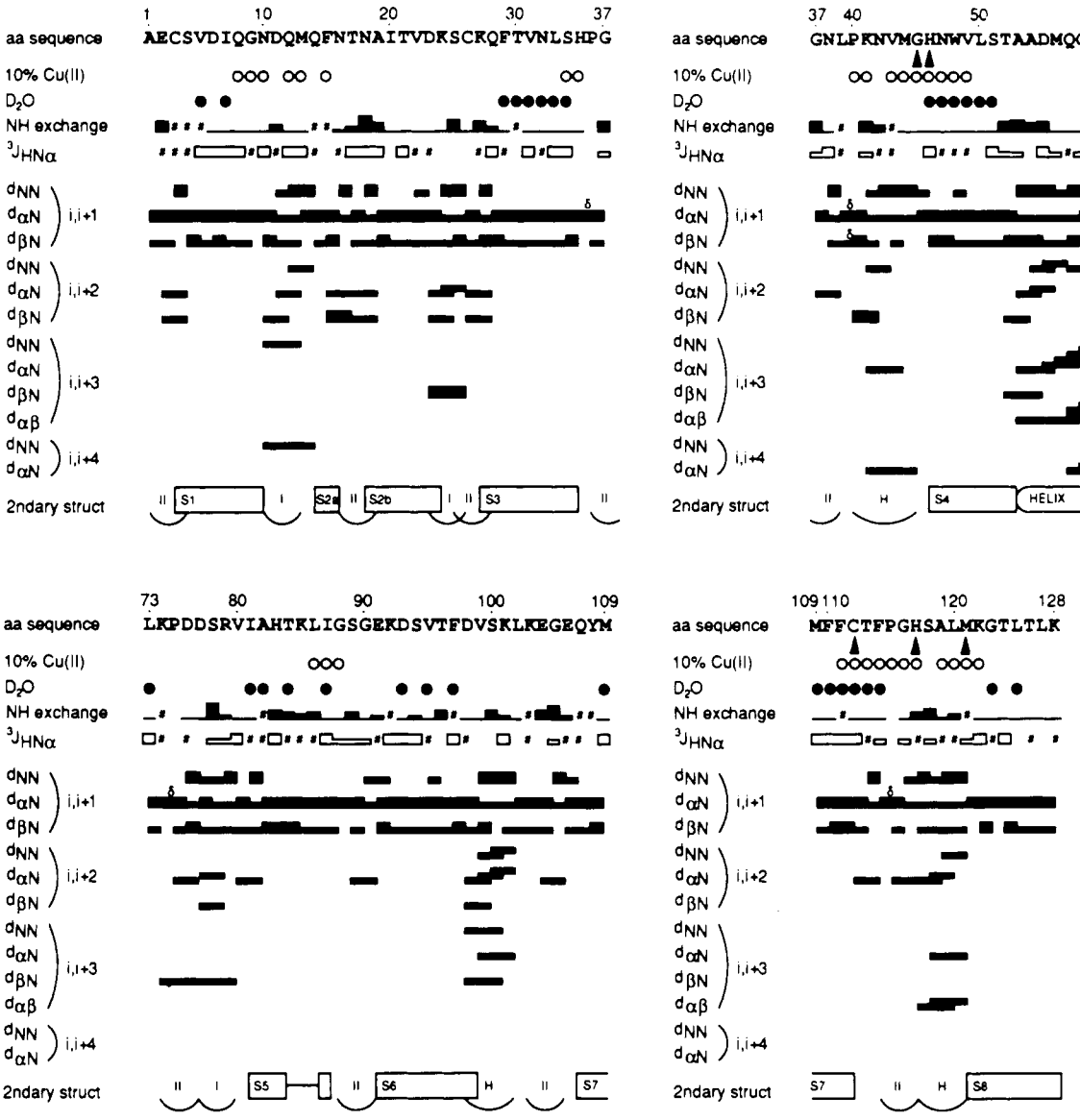

FIGURE 5: Observed short- and medium-range sequential NOEs. Intensities were derived from NOESY spectra with τ_{mix} = 100 ms and classified relative to the usual strength of an intraresidue $d_{N\alpha}(i,i)$ NOE ($d = 2.9 \pm 0.1$ Å), with thick bars representing equally strong or stronger NOEs ($d \leq 2.9$ Å) and thin bars representing weaker NOEs ($d > 2.9$ Å). The upper line shows the amino acid sequence, in which Cu ligand residues are marked with an arrowhead. The second line [denoted by 10% Cu(II)] indicates the residues (denoted by O) for which broadening is observed of their NH–C$^{\alpha}$H cross peaks in the COSY spectrum that was recorded for a partially oxidized [10% Cu(II)] azurin sample. The third line (denoted by D_2O) indicates residues (denoted by ●) whose NH–C$^{\alpha}$H cross peaks are observed in COSY and HOHAHA spectra for azurin in D_2O and whose NHs thus exchange very slowly (time scale of hours to days). The fourth line indicates the relative rates of NH exchange according to the number of contour levels of ^{15}NH–H_2O exchange cross peaks in the 3D $^1H\{^{15}N\}$ NOESY-HSQC spectrum that was recorded without water presaturation. The height of the bars (1–9 contour levels) increases with increasing exchange rates (approximately 1–100 s^{-1}); when only the baseline is given (no ^{15}NH–H_2O cross peak observed), NH exchange is slower than approximately 0.1 s^{-1}. The fifth line contains $^3J_{HN\alpha}$ estimates (low bars < 6 Hz, high bars > 8 Hz). A # mark in the fourth and fifth lines indicates that the determination of the NH exchange or the $^3J_{HN\alpha}$ coupling constant was impaired by overlap. In the bottom line, secondary structure elements are denoted (see also Figure 6).

from interstrand NOEs in which Ile-87 is involved and from the lack of interstrand NOEs with Lys-85 and Leu-86 main-chain protons.

(*b*) *Helix.* From residues Ala-53 to Gly-67, a helix is present. NOE connectivities were observed between Gly-63 C$^{\alpha}$H and Leu-73 C$^{\alpha}$H and Lys-74 NH resonances, the latter two residues being part of a large loop which bends back from the end of the helix to the β-core.

(*c*) *Turns and Loops.* Most loop regions that interconnect the β-strand and helix elements are structurally well defined. They contain 11 tight turns and 4 helical turns. In addition, a tight turn is present at the N-terminus. The loop between the helix and β-strand S5 consists of four consecutive turns (one helical turn, followed by three tight turns). A long-range $d_{\alpha N}$(71,86) NOE suggests the packing of the tight turn between Lys-70 and Leu-73 onto the β-core of the protein. On the basis of NOE information only, the tight turns were tentatively classified as belonging to the type I family (consisting of type I and I′ turns) or as belonging to the type II family (consisting of the type II, II′, and half-turns) (Richardson, 1981; Wüthrich, 1986).

All helical turns are located in long loops that contain at least an additional tight turn or a region with an extended conformation. An example of such a loop is the Cu ligand loop between residues Cys-112 and Met-121, which consists of a tight turn followed by a helical turn. For this helical turn, two $d_{\alpha\beta}(i,i+3)$ NOEs are observed, indicative of a α-helical conformation. Three $d_{\alpha N}(i,i+2)$ NOEs are observed

Table II: ^{15}N and ^{1}H Chemical Shifts (ppm) for Wild-Type Reduced Cu(I) Azurin from *P. aeruginosa* at pH 5.5 and 40 °C, in 25 mM Potassium Phosphate[a]

residue	amide NH ^{15}N	amide NH ^{1}H	$C^{\alpha}H$ ^{1}H	$C^{\beta}H$ ^{1}H	other ^{1}H (^{15}N)
Ala-1			4.12	1.44	
Glu-2	124.7	8.86	4.51	2.20, 2.07	$C^{\gamma}H$ 2.37
Cys-3	120.5	8.72	5.05	4.14, 2.79	
Ser-4	113.1	7.22	4.62	3.38, 3.29	
Val-5	118.9	8.07	4.42	2.09	$C^{\gamma}H_3$ 0.95, 0.79
Asp-6	126.3	8.12	5.31	2.53, 2.49	
Ile-7	124.4	8.97	4.80	1.29	$C^{\gamma 2}H_3$ 0.52; $C^{\gamma 1}H$ *1.11, 0.86*; $C^{\delta 1}H_3$ *0.10*
Gln-8	123.6	8.32	5.30	1.73, *1.63*	$C^{\gamma}H$ *2.29, 2.26*; $N^{\epsilon 2}H$ 7.38, 6.60 (110.4)
Gly-9	108.5	8.55	5.18, 2.75		
Asn-10	122.4	7.60	5.26	3.68, 2.80	$N^{\delta 2}H$ 7.35, 7.05 (110.8)
Asp-11	119.3	8.37	4.99	3.00, 2.79	
Gln-12	117.0	7.56	4.39	1.79, 1.77	$C^{\gamma}H$ 2.29, 2.17; $N^{\epsilon 2}H$ 7.46, 6.62 (112.0)
Met-13	113.5	7.27	3.41	2.19, 2.16	$C^{\gamma}H$ 1.87, 1.64; $C^{\epsilon}H_3$ 1.99
Gln-14	109.3	6.62	4.65	1.97, 1.69	$C^{\gamma}H$ 2.31, 2.24; $N^{\epsilon 2}H$ 7.28, 6.69 (110.8)
Phe-15	120.9	8.85	6.20	3.40, 3.29	$C^{\delta}H$ 7.25; $C^{\epsilon}H$ 7.14; $C^{\zeta}H$ 8.09
Asn-16	117.0	8.74	4.70	3.27, 2.79	$N^{\delta 2}H$ 7.73, 7.14 (114.3)
Thr-17	112.4	7.17	4.78	4.17	$C^{\gamma 2}H_3$ 0.99
Asn-18	121.6	8.46	5.15	3.22, 3.15	$N^{\delta 2}H$ 7.60, 6.95 (110.4)
Ala-19	124.0	8.30	5.53	1.38	
Ile-20	122.8	9.01	4.48	1.49	$C^{\gamma 2}H_3$ 0.81; $C^{\gamma 1}H$ *1.48, 0.93*; $C^{\delta 1}H_3$ *0.25*
Thr-21	124.4	8.72	4.97	3.94	$C^{\gamma 2}H_3$ 1.08
Val-22	127.8	8.86	3.65	1.56	$C^{\gamma}H_3$ 0.37, –0.32
Asp-23	128.2	8.15	4.77	3.01, 2.64	
Lys-24	125.9	8.86	3.95	1.90, 1.69	$C^{\gamma}H$ *1.37*; $C^{\delta}H$ *1.58*; $C^{\epsilon}H$ 2.95
Ser-25	115.1	8.97	4.30	3.94, 3.89	
Cys-26	122.8	8.27	4.48	3.34, 3.11	
Lys-27	122.4	8.73	4.27	1.90, 1.72	$C^{\gamma}H$ *1.52*; $C^{\delta}H$ *1.61*; $C^{\epsilon}H$ 3.04
Gln-28	116.6	7.78	5.01	1.74, 1.71	$C^{\gamma}H$ 2.26, 2.17; $N^{\epsilon 2}H$ 7.37, 6.69 (111.6)
Phe-29	121.6	8.42	4.91	1.98, 1.62	$C^{\delta}H$ 6.76; $C^{\epsilon}H$ 7.09; $C^{\zeta}H$ 6.88
Thr-30	122.8	7.05	5.10	3.33	$C^{\gamma 2}H_3$ 0.78
Val-31	125.9	8.63	3.87	0.97	$C^{\gamma}H$ –0.22, –0.67
Asn-23	125.1	8.37	5.00	3.05, 2.54	$N^{\delta 2}H$ 7.17, 6.55 (115.1)
Leu-33	128.2	9.12	5.41	1.98, 1.96	$C^{\gamma}H$ *1.68*; $C^{\delta}H_3$ *1.02, 0.97*
Ser-34	119.7	8.73	5.10	4.06, 3.89	
His-35	118.2	8.62	6.51	3.73, 2.68	$C^{\epsilon 1}H$ 9.37; $C^{\delta 2}H$ 7.32
Pro-36			4.87	2.48, 1.98	$C^{\gamma}H$ 2.05; $C^{\delta}H$ 3.78, 3.49
Gly-37	110.8	8.61	4.98, 3.69		
Asn-38	119.3	11.30	4.99	2.74, 2.58	$N^{\delta 2}H$ 7.45, 6.73 (112.4)
Leu-39	123.6	8.62	4.68	*1.90*	$C^{\gamma}H$ *1.81*; $C^{\delta}H_3$ *1.02, 0.98*
Pro-40			4.79	2.37, 2.28	$C^{\gamma}H$ *2.20*, 1.99; $C^{\delta}H$ 3.88, 3.45
Lys-41	119.7	8.98	3.50	1.72, 1.68	$C^{\gamma}H$ *1.14*; $C^{\delta}H$ *1.45*; $C^{\epsilon}H$ 3.05
Asn-42	109.3	8.22	4.65	2.98, 2.77	$N^{\delta 2}H$ 7.61, 6.81 (113.5)
Val-43	115.8	7.17	4.52	1.91	$C^{\gamma}H_3$ 1.05, 0.98
Met-44	120.9	7.86	4.22	1.91, 1.88	$C^{\gamma}H$ 1.55, 1.46; $C^{\epsilon}H_3$ 2.04
Gly-45	115.1	5.92	4.14, 3.23		
His-46	111.2	8.22	7.25	3.32, 2.35	$C^{\epsilon 1}H$ 6.87; $C^{\delta 2}H$ 5.55; $N^{\epsilon 2}H$ 11.50 (160.6)
Asn-47	124.4	10.58	4.73	2.65, 2.38	$N^{\delta 2}H$ 7.68, 5.80 (105.8)
Trp-48	113.5	7.41	4.65	3.28, 2.80	$C^{\delta 1}H$ 6.05; $C^{\zeta 2}H$ 6.52; $C^{\eta 2}H$ 6.69; $C^{\zeta 3}H$ 6.41; $C^{\epsilon 3}H$ 7.40; $N^{\epsilon 1}H$ 6.10 (123.2)
Val-49	129.0	8.16	3.99	1.08	$C^{\gamma}H_3$ 0.93, 0.65
Leu-50	124.0	7.50	4.85	1.34, *0.68*	$C^{\gamma}H$ *1.15*; $C^{\delta}H_3$ *0.88, 0.22*
Ser-51	122.4	9.17	5.06	4.10, 3.72	
Thr-52	111.6	9.92	4.84	4.72	$C^{\gamma 2}H_3$ 1.43
Ala-53	125.9	8.90	3.88	1.37	
Ala-54	118.6	8.28	4.07	1.39	
Asp-55	115.8	7.31	4.71	2.78, 2.72	
Met-56	120.1	7.00	3.60	1.75, 1.54	$C^{\gamma}H$ 1.34, 0.77; $C^{\epsilon}H_3$ 1.67
Gln-57	115.8	8.56	3.74	1.96, 1.92	$C^{\gamma}H$ 2.32; $N^{\epsilon 2}H$ 7.45, 6.72 (112.4)
Gly-58	110.0	8.40	3.79, 3.79		
Val-59	122.0	7.91	3.60	2.27	$C^{\gamma}H_3$ 1.04, 1.01
Val-60	120.1	8.43	3.57	2.06	$C^{\gamma}H_3$ 0.96, 0.71
Thr-61	117.8	8.51	3.90	4.27	$C^{\gamma 2}H_3$ 1.26
Asp-62	122.0	8.50	4.59	2.75, 2.64	
Gly-63	113.5	8.62	4.14, 3.51		
Met-64	122.0	8.18	4.04	2.45, 2.25	$C^{\gamma}H$ 2.55; $C^{\epsilon}H_3$ 2.09
Ala-65	117.4	7.05	4.21	1.53	
Ser-66	114.7	7.65	4.27	3.87, 3.75	
Gly-67	102.7	6.73	4.22, 3.59		
Leu-68	122.4	7.91	2.89	*1.48*	$C^{\gamma}H$ *0.94*
Asp-69	116.6	8.50	4.35	2.65, 2.68	
Lys-70	118.9	6.86	4.52	*1.39*, 1.31	$C^{\gamma}H$ *2.48*; $C^{\delta}H$ *1.65*; $C^{\epsilon}H$ 3.04
Asp-71	115.1	7.96	3.98	3.06, 3.01	
Tyr-72	105.4	7.66	3.64	3.07, 2.43	$C^{\delta}H$ 6.98; $C^{\epsilon}H$ 6.50
Leu-73	117.4	7.05	4.59	1.34, *1.14*	$C^{\gamma}H$ *1.48*; $C^{\delta}H_3$ *0.77, 0.44*

Table II: (Continued)

residue	amide NH ^{15}N	amide NH ^{1}H	$C^{\alpha}H$ ^{1}H	$C^{\beta}H$ ^{1}H	other ^{1}H (^{15}N)
Lys-74	127.1	8.87	4.58	*1.91*	$C^{\gamma}H$ *1.44*
Pro-75			4.22	2.30, 2.27	$C^{\gamma}H$ 2.13, 1.94; $C^{\delta}H$ 4.16, 3.63
Asp-76	118.9	8.71	4.30	2.89, 2.70	
Asp-77	117.4	7.27	4.27	2.96, 2.92	
Ser-78	125.1	8.62	4.30	4.09, 4.00	
Arg-79	119.7	8.56	4.18	1.83, 1.80	$C^{\gamma}H$ 1.64; $C^{\delta}H$ 3.37, 2.86; $N^{\epsilon}H$ 8.92 (84.9); $N^{\eta}H$ 6.48 (71.1)
Val-80	118.2	7.32	3.92	2.31	$C^{\gamma}H_3$ 1.38, 0.90
Ile-81	132.1	8.89	3.72	1.16	$C^{\gamma 2}H_3$ 0.53; $C^{\gamma 1}H$ *1.74*; $C^{\delta 1}H_3$ *0.85*
Ala-82	116.6	7.17	4.74	1.12	
His-83	113.1	8.56	6.19	3.40, 3.33	$C^{\epsilon 1}H$ 8.69; $C^{\delta 2}H$ 7.25
Thr-84	110.4	8.81	4.79	5.20	$C^{\gamma 2}H_3$ 1.29; $O^{\gamma 1}H$ 5.45
Lys-85	121.6	9.31	4.74	1.90, *1.53*	$C^{\gamma}H$ *1.48*; $C^{\delta}H$ *1.79*; $C^{\epsilon}H$ 3.12
Leu-86	120.5	8.01	4.79	1.97, *1.32*	$C^{\gamma}H$ *1.41*; $C^{\delta}H_3$ *1.11*, *1.00*
Ile-87	121.3	9.72	4.88	2.18	$C^{\gamma 2}H_3$ 0.77; $C^{\gamma 1}H$ *1.66*
Gly-88	110.0	9.19	4.11, 3.52		
Ser-89	110.4	6.80	3.95	3.35, 3.35	
Gly-90	110.8	8.43	4.18, 3.77		
Glu-91	118.9	7.52	4.70	2.55, 2.52	$C^{\gamma}H$ 2.29, 2.13
Lys-92	117.0	8.21	5.24	1.84, 1.79	$C^{\gamma}H$ *1.38*, *1.32*; $C^{\delta}H$ *1.59*; $C^{\epsilon}H$ 2.92
Asp-93	117.8	8.99	5.11	2.76, 2.25	
Ser-94	115.8	8.02	5.73	3.65, 3.56	
Val-95	122.0	8.66	4.71	1.89	$C^{\gamma}H_3$ 1.10, 0.83
Thr-96	124.7	8.42	5.40	3.69	$C^{\gamma 2}H_3$ 0.94
Phe-97	122.8	8.81	5.30	3.12, 2.93	$C^{\delta}H$ 6.88; $C^{\epsilon}H$ 6.90; $C^{\zeta}H$ 6.79
Asp-98	120.5	8.56	4.78	2.92, 2.65	
Val-99	127.5	7.86	3.45	1.90	$C^{\gamma}H_3$ 0.87, 0.54
Ser-100	115.5	8.60	4.34	4.08, 3.99	
Lys-101	119.7	7.46	4.21	1.94, *1.84*	$C^{\gamma}H$ *1.02*; $C^{\delta}H$ *1.70*; $C^{\epsilon}H$ 3.19
Leu-102	118.6	7.93	4.47	2.01, 1.06	$C^{\gamma}H$ 1.48; $C^{\delta}H_3$ 0.64, –0.03
Lys-103	120.5	8.72	4.65	*1.90*, 1.74	$C^{\gamma}H$ *1.48*; $C^{\delta}H$ *1.72*; $C^{\epsilon}H$ 2.99
Glu-104	125.1	8.88	4.18	2.06, 2.00	$C^{\gamma}H$ 2.37, 2.30
Gly-105	112.7	8.94	4.25, 3.81		
Glu-106	120.5	7.18	4.48	1.82, 1.72	$C^{\gamma}H$ 1.92, 1.88
Gln-107	124.7	9.19	4.68	2.07, 1.96	$C^{\gamma}H$ 2.36, 2.29; $N^{\epsilon 2}H$ 7.24, 6.74 (111.2)
Tyr-108	124.0	8.55	4.93	3.32, 2.99	$C^{\delta}H$ 6.94; $C^{\epsilon}H$ 6.93
Met-109	120.5	9.09	5.61	*2.38*, 1.70	$C^{\gamma}H$ *2.68*, *2.30*; $C^{\epsilon}H_3$ 1.95
Phe-110	117.0	8.43	6.03	2.00, 1.58	$C^{\delta 1}H$ 6.75; $C^{\epsilon 1}H$ 7.34; $C^{\zeta}H$ 7.00; $C^{\epsilon 2}H$ 6.67; $C^{\delta 2}H$ 6.51
Phe-111	115.5	7.88	5.43	3.54, 2.86	$C^{\delta}H$ 6.55; $C^{\epsilon}H$ 7.05; $C^{\zeta}H$ 6.85
Cys-112	121.3	7.04	5.74	3.40, 2.86	
Thr-113	118.9	9.99	4.57	4.96	$C^{\gamma 2}H_3$ 1.40; $O^{\gamma 1}H$ 5.66
Phe-114	134.8	10.48	3.44	2.63, 2.47	$C^{\delta}H$ 6.55; $C^{\epsilon}H$ 7.36; $C^{\zeta}H$ 7.07
Pro-115			3.87	*1.85*, *1.59*	$C^{\gamma}H$ *1.56*; $C^{\delta}H$ 3.85
Gly-116	111.6	8.55	4.45, 3.76		
His-117	122.0	8.83	4.84	3.67, 3.36	$C^{\epsilon 1}H$ 6.79; $C^{\delta 2}H$ 6.89; $N^{\epsilon 2}H$ 11.55 (163.3)
Ser-118	116.6	9.60	*4.25*	*4.45*, *3.77*	
Ala-119	122.0	7.16	4.11	1.41	
Leu-120	114.3	7.44	4.70	1.85	
Met-121	123.2	9.06	4.27	*2.22*, 1.70	$C^{\gamma}H$ *1.44*; $C^{\epsilon}H_3$ – 0.05
Lys-122	116.2	7.21	5.68	2.24, 1.68	$C^{\gamma}H$ *1.21*, *1.17*; $C^{\delta}H$ *1.48*; $C^{\epsilon}H$ 2.97
Gly-123	110.0	8.29	4.15, 3.12		
Thr-124	109.3	7.84	5.22	4.28	$C^{\gamma 2}H_3$ 1.35
Leu-125	125.1	8.08	5.72	1.59, 1.56	$C^{\gamma}H$ *1.46*; $C^{\delta}H_3$ *0.88*, *0.57*
Thr-126	120.1	8.41	4.89	4.07	$C^{\gamma 2}H_3$ 1.32
Leu-127	127.1	8.77	5.16	1.64, 1.38	$C^{\gamma}H$ *1.42*; $C^{\delta}H_3$ *0.76*
Lys-128	130.2	8.55	4.35	1.72, 1.61	$C^{\gamma}H$ *1.35*; $C^{\delta}H$ *1.38*; $C^{\epsilon}H$ 3.00

[a] ^{1}H chemical shifts (±0.02 ppm) are expressed relative to DSS; ^{15}N chemical shifts (±0.2 ppm) are referenced to liquid ammonia. Chemical shifts in italics indicate that the positions of the corresponding protons in the amino acid residues are determined exclusively via HOHAHA spectra; these positions are to be regarded as tentative. Underlined chemical shifts refer to protons whose positions in the amino acid side chain were determined exclusively via NOESY spectra.

in each of the helical turns between positions 67–71 and 98–102, indicative of 3_{10}-helical conformation. The helical turn between positions 40 and 45 is probably less regular.

Main-Chain NH Exchange. Main-chain NH exchange data were obtained from two different experimental approaches. In the first approach, the more slowly exchanging NHs (i.e., which exchange on the time scale of hours to days) were identified by the observation of NH–$C^{\alpha}H$ cross peaks in the 2D DQF-COSY and HOHAHA spectra that were recorded for a D_2O-exchanged sample. A total of 33 tightly bound amide protons were detected by this approach (Figures 1C and 5). In the second approach, exchange rates of the faster exchanging NHs (i.e., which exchange faster than 1 s^{-1}) were derived from the intensities of ^{15}NH–H_2O cross peaks that were observed in the 3D $^{1}H\{^{15}N\}$ NOESY-HSQC spectrum, which was recorded without using presaturation of the water signal. The absence of such a ^{15}NH–H_2O cross peak indicates that NH exchange is slower than approximately 0.1 s^{-1}. Reliable assignment of cross peaks at the H_2O line position as ^{15}NH–H_2O cross peaks was facilitated by the

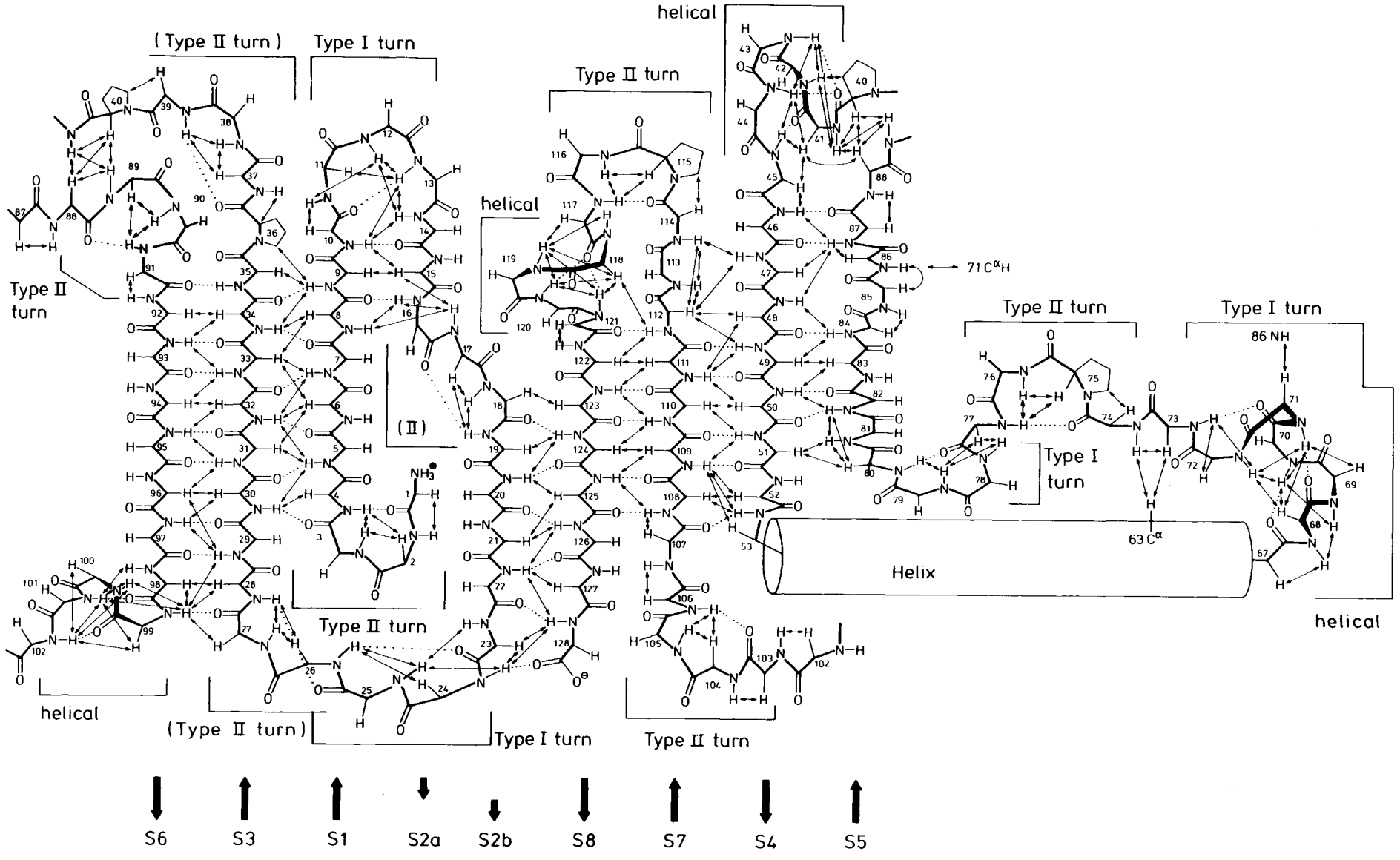

FIGURE 6: Secondary structure of reduced Cu(I) azurin in solution. Arrows denote observed medium- and long-range NOEs (in spectra with τ_{mix} = 100 ms). In the turns and loops, the principal sequential NOEs (that underly turn classification) are indicated also. H-bonds are depicted by dotted lines. The numbering of β-strands is according to the numbering in the secondary structure of azurin in the crystal (Nar et al., 1991a). Two families of tight turns are distinguished, type I (consisting of type I and I′ turns) and type II (consisting of type II, II′, and half-turns). Turns that are differently categorized in the crystal structure are in brackets (see Discussion).

virtually complete assignment of the cross peaks in the 3D $^1H\{^{15}N\}$ spectrum. When a $^{15}NH-H_2O$ cross peak overlapped with another NOE cross peak, no NH exchange rate could be determined (this is denoted by a # mark on the NH exchange line in Figure 5). By using the second approach, clear variations were observed among the NH exchange rates of the 91 amide protons that were not observed in the 2D D_2O spectra (Figure 5). A discrepancy is observed for Thr-84. The observation of its NH resonance in the D_2O spectra would indicate that its amide proton exchanges on the time scale of hours to days. However, the observation of a cross peak between its ^{15}NH resonance and the H_2O signal in the NOESY-HSQC spectrum would indicate that the Thr-84 NH exchanges faster than 1 s^{-1}. This is discussed more fully under Discussion.

In general, exchange of the main-chain amide protons that are involved in H-bonding in the β-sheets takes place on a time scale of hours to days; nearly all main-chain amide protons whose resonances are observed in the 2D D_2O spectra occur in the central β-strands or are H-bonded to these strands. NH exchange in the helix takes place on a time scale which ranges from tens of milliseconds to hours/days; only the Val-59 and -60 NHs exchange on the hours to days time scale, as shown by the observation of their NH–$C^\alpha H$ cross peaks in D_2O spectra. The time scale of the exchange of the main-chain amide protons of the residues that occur at the $i+3$ position in tight turns and which thus are H-bonded to the main-chain C=O group of residue i ranges from tens of milliseconds for the His-117 NH to hours/days for the Leu-73 NH. Amide protons that presumably are involved in H-bonding in helical turns exchange generally on a time scale of hundreds of milliseconds to hours. It can be concluded that the observed hydrogen exchange pattern is compatible with and supports the presence of the inferred main-chain H-bonds in the deduced secondary structure of azurin. It is clear, however, that the proposed H-bonds do not suffice to explain all NH exchange data, like the relatively slow exchange of the NHs of Asn-47, Trp-48, Tyr-72, Thr-113, and Phe-114.

Cu Oxidation. Thirty-three NH–$C^\alpha H$ cross peaks ($C^\alpha H$–$C^\beta H$ for Pro) in the 2D DQF-COSY spectrum recorded for 90% diamagnetic Cu(I)/10% paramagnetic Cu(II) azurin were broadened relative to the NH–$C^\alpha H$ cross peaks in the 2D DQF-COSY spectrum of fully reduced [100% Cu(I)] azurin (Figures 1A,B and 5), indicating the proximity of either one or both of the corresponding protons to the Cu ion (Canters et al., 1984b). Broadening of NH–$C^\alpha H$ cross peaks was observed among others for all Cu ligand residues except Gly-45 and for all residues in the Cu ligand loop (Cys-112–Met-121) except Ser-118. Gly-45 and Ser-118 are exceptions, because they have no observable NH–$C^\alpha H$ cross peaks in the DQF-COSY spectrum recorded for reduced azurin. However, the Gly-45 NH resonance at 5.92 ppm (Figure 1A,B) and the Ser-118 $C^\alpha H$–$C^\beta H$ cross peaks were broadened in the the DQF-COSY spectrum recorded for partially oxidized azurin relative to the spectrum of fully reduced azurin.

DISCUSSION

Sequential Assignments. By using a combination of 2D and 3D homonuclear and heteronuclear NMR spectroscopic experiments, complete sequential main-chain and nearly complete side-chain resonance assignments were obtained for reduced wt azurin at pH 5.5 and 40 °C in aqueous solution. The recorded 3D ^1H HOHAHA-NOESY spectrum proved to be very valuable for this. First, its analysis provided for complete sequential assignments. Second, it allowed for the unambiguous assignment of virtually all NOE connectivities observed in a 3D $^1H\{^{15}N\}$ NOESY-HSQC spectrum. Third, it enabled the recognition of secondary structure elements by its combined content of J coupling and NOE information (Oschkinat et al., 1990). The 3D $^1H\{^{15}N\}$ NOESY-HSQC spectrum that was recorded without water presaturation was useful, not only because of its high resolving power but also because it provided for NH exchange data that were complementary to the information obtained from 2D spectra recorded for a sample in D_2O.

Comparison of the reported assignments with previously obtained partial assignments shows that most of the latter ones are correct. These include resonance assignments to the ligand His-46 and -117 $C^{\delta 2}H$ and $C^{\epsilon 1}H$ and ligand Met-121 $C^\epsilon H_3$ protons, to most of the upfield-shifted CH ($\delta < 0.5$ ppm), and to all the other Met $C^\epsilon H_3$ protons (Adman et al., 1982; Canters et al., 1984a,b; Van de Kamp et al., 1990a,c).

Secondary Structure. From the reported NMR data, a well-defined secondary structure for reduced azurin in solution emerges (Figure 6). This structure is compared below with the secondary structure elements in the X-ray crystal structure of wt *P. aeruginosa* azurin [resolution of 1.9 Å (Nar et al., 1991b); see also Figure 3 in Nar et al. (1991a)] obtained for the oxidized protein at pH 5.5 and 4 °C.

(*a*) *β-Sheet.* The NMR secondary structure contains two β-sheets. No differences are found with the crystal structure.

(*b*) *Helix.* In the NMR-derived secondary structure, a helix is present between Ala-53 and Gly-67. In the crystal structure, this helix consists of a central α-helical region (Asp-55–Gly-63) preceded and followed by turns with 3_{10} character. The presence of $d_{\alpha N}(i,i+4)$ NOEs and the absence of $d_{\alpha N}(i,i+2)$ NOEs in the region 55–64 and the presence of $d_{\alpha N}(i,i+2)$ NOEs and the absence of $d_{\alpha N}(i,i+4)$ NOEs in the regions 53–55 and 64–67 indicate that in solution the helix consists of similar 3_{10}–α–3_{10} regions.

(*c*) *Turns and Loops.* Azurin in solution contains a high number of tight and helical turns. Comparison with the crystal structure shows that all turns that were classified as belonging to the type I family in solution (Figures 5 and 6) in the crystal are of type I and I′. In the crystal the turn between Lys-70 and Leu-73 is the only type I′ turn. It is interesting to note that in solution a similar type I′ conformation of this turn is indicated by the observation of strong intraresidue $d_{N\alpha}(i,i)$ NOEs for Asp-71 and Tyr-72 (the intraresidual NH–$C^\alpha H$ distance is 2.3 Å for the second and third residue in a type I′ turn). Furthermore, the turns between residues 1–4, 74–77, 88–91, 103–106, and 114–117 that were classified as belonging to the type II family in solution (Figures 5 and 6) in the crystal are of type II. In solution, a similar type II conformation of these turns is indicated by the observation of strong $d_{N\alpha}(i,i)$ NOEs for the third residues of these turns (the intraresidual NH–$C^\alpha H$ distance is 2.3 Å for the third residue in a type II turn). In summary, for the aforementioned tight turns no differences are indicated with the crystal structure, not even for turns that have high crystallographic temperature (B) factors or that might be perturbed by crystal packing effects (Nar et al., 1991a,b). However, three other turns were differently classified in solution than in the crystal. In solution, the turns between residues 16–19, 25–28, and 36–39 were tentatively classified as belonging to the type II family (Figures 5 and 6), but the crystal structure lacks the corresponding $C{=}O_i\cdots HN_{i+3}$ H-bonds; instead the latter shows two type VIII turns (Wilmot & Thornton, 1990) at positions 15–18 and 26–29 and an extended conformation between residues 36 and 40. The presence of tight turns in solution can only

be achieved by major adjustments relative to the crystal structure at these positions. Definite conclusions must await further analysis of the solution structure.

No differences could be detected that might have to do with differences in oxidation state between the solution [Cu(I); NMR] and the crystal [Cu(II); X-ray] structure. Evidence for the integrity of the disulfide bridge between Cys-3 and Cys-26 in the reduced protein is derived from the observation of weak $d_{\beta\beta}(3,26)$, $d_{\alpha\beta}(3,26)$, and $d_{\beta\alpha}(3,26)$ NOEs and by the observation of similar NH exchange rates in this region for the oxidized and the reduced protein from 1D ^{1}H NMR D_2O exchange studies (data not shown).

In summary, the secondary structures of Cu(I) azurin in solution and Cu(II) azurin in the crystalline state seem to be virtually identical.

NH Exchange. Relative main-chain NH exchange rates were obtained for 111 out of 128 residues (four residues are Pro's; for 13 other residues no NH–C$^\alpha$H cross peak was observed in the D_2O spectra and observation of NH exchange in the 3D ^{1}H{^{15}N} NOESY-HSQC spectrum was prohibited by overlap). Full analysis of these exchange data in terms of main- and side-chain H-bonding and solvent accessibility will be given elsewhere. Here a few points of interest are discussed. These points are the Thr-84 NH exchange rate, the main-chain NH exchange rates in the Cu ligand loop, and the exchange of the His imidazole NHs. The discussion is based on the assumption that the three-dimensional structures in solution and in the crystal are identical. Evidence to validate this assumption will be given elsewhere.

(a) Thr-84. In all cases where a main-chain NH resonance was observed in the 2D D_2O spectra (exchange rate $\leq 1 \times 10^{-4}$ s^{-1}), no ^{15}NH–H_2O exchange cross peak was detected in the 3D ^{1}H{^{15}N} NOESY-HSQC spectrum that was recorded without water presaturation, with the exception of Thr-84 (Figure 5). While the Thr-84 NH resonance was clearly observed in the D_2O spectra, a rather intense Thr-84 ^{15}NH–H_2O cross peak was also detected in the NOESY-HSQC spectrum. We favor the explanation that this cross peak is not the result of Thr-84 NH exchange but arises from NOE transfer to an exchangeable proton in its vicinity. According to the crystal structure and in view of the reported assignments, the only proton which might give rise to such an NOE peak at the waterline is His-83 N$^{\delta 1}$H. No resonance could be assigned to His-83 N$^{\delta 1}$H, probably due to fast exchange with H_2O. The Thr-84 ^{15}NH–H_2O cross peak might result then from a direct NOE with His-83 N$^{\delta 1}$H which is in exchange with H_2O (Van de Ven et al., 1988).

(b) Cu Ligand Loop. Main-chain NH exchange of the first three residues in the Cu ligand loop (Cys-112, Thr-113, and Phe-114) is so slow that their NH resonances are visible in the 2D D_2O spectra (time scale of hours to days). Such slow NH exchange can be explained by the presence of the following H-bonds, as observed in the X-ray crystal structure: Cys-112 NH···O=C Met-121, Thr-113 NH···O$^{\delta 1}$ Asn-47, and Phe-114 NH···S$^\gamma$ Cys-112. Cys-112 S$^\gamma$, which coordinates the Cu ion, is also the H-bond acceptor of Asn-47 NH, which is visible in the 2D D_2O spectra too. Apparently, these are all strong H-bonds. The Phe-114 NH···S$^\gamma$ Cys-112 and the Asn-47 NH···S$^\gamma$ Cys-112 H-bonds might play a role in determining the spectral and redox properties of the Cu site.

The present finding of very slow Asn-47 and Phe-114 NH exchange has some implications for the interpretation of the resonance Raman (RR) spectra of azurins and other blue copper proteins. In the past, it has been observed that most of the vibrational modes in the RR spectra undergo shifts of 1–2 cm^{-1} in D_2O, and this phenomenon has been ascribed to spectral contributions from the His–imidazole ligands (Nestor et al., 1984; Blair et al., 1985) or to H-bonding of the Cys–S$^\gamma$ ligand (Ainscough et al., 1987; Mino et al., 1987; Han et al., 1991). The extremely slow rate of exchange of Asn-47 and Phe-114 NHs under conditions similar to those used for the RR experiments makes it unlikely, at least in the case of azurin, that the deuterium isotope effect is due to H-bonding of the sulfur ligand.

The involvement of Cys-112, Thr-113, Phe-114, and Asn-47 NHs in strong H-bonding confers considerable rigidity to this part of the Cu-binding site. That the Cu site is rigid has previously been inferred from crystallographic analysis. It has been shown that the X-ray structures of the Cu sites of the *P. aeruginosa* and *Alcaligenes denitrificans* azurins are roughly independent of the Cu oxidation state and have relatively low crystallographic *B* factors (Baker, 1988; Shepard et al., 1991; Nar et al., 1991a,b; H. Nar, unpublished results). Moreover, even upon metal substitution or complete removal of the Cu ion, the structures of the metal and apo- sites resemble those of the Cu sites in the holoproteins (Baker et al., 1991; Nar et al., 1992a,b). A rigid Cu site has been thought to be a prerequisite for fast electron transfer.

It has to be noted, however, that the main-chain NHs of different residues in the Cu ligand loop (Cys-112–Met-121) exchange with different rates; e.g., the main-chain NHs of residues 117–120 are exchanging on a faster time scale (of tens to hundreds of milliseconds) than the NHs of the residues 112–114 (Figures 3 and 5), indicating the absence of strong H-bonding. Thus, the region comprising the residues 117–120 might be more flexible. Some mobility of the Cu site is furthermore indicated by the observation that the Phe-15 and Phe-114 aromatic rings, which flank the Cu ligand residues Met-121 and His-117, respectively, are flipping rapidly on the NMR time scale. Thus, the NMR data do not support the idea that the proposed rigidity is a uniform property of the full Cu-binding site of the protein in solution.

(c) Imidazole NH Exchange. Among the assignment of resonances to side-chain NHs, the observation of the N$^{\epsilon 2}$H resonances from the Cu ligand residues His-46 and -117 is especially interesting. According to the crystal structure, the observation of the His-46 N$^{\epsilon 2}$H resonance can be understood from the buried, H-bonded (to Asn-10 C=O), water-inaccessible position of the His-46 N$^{\epsilon 2}$H proton (Nar et al., 1991a,b). The His-117 N$^{\epsilon 2}$H proton, on the other hand, is fully exposed to the solvent and is not in H-bonding contact with any protein atom. This would usually make detection of its resonance impossible, due to fast exchange with bulk water. A possible explanation for the slow exchange of the His-117 N$^{\epsilon 2}$H proton is that the protein conformation around His-117 is different in solution when compared to the crystal structure. However, this explanation is discarded as all observed NOEs with the His-117 imidazole protons are in agreement with the X-ray structure.

An alternative explanation is based on the observation that in the crystal structure His-117 N$^{\epsilon 2}$H appears to be H-bonded to a surface water molecule with a low crystallographic *B* factor (Nar et al., 1991a,b). Binding of this water molecule to the His-117 N$^{\epsilon 2}$H proton (Nar et al., 1991a) might impair fast exchange of this proton. This possibility gains additional interest in view of the fact that electron transfer to and from the Cu most probably is mediated by His-117 (Van de Kamp et al., 1990a,b). Binding of a water molecule to His-117 might be of functional importance for electron transfer via His-117, e.g., by providing the protein with a facilitated electron transfer

pathway (Nar et al., 1991a), or by enabling a coupled electron and proton transfer event. However, recent NMR reports of Otting et al. (1990, 1991a,b,c) indicate that hydration of a protein surface is effected by water molecules with residence times in the subnanosecond range, even when they are located in hydration sites that contain well-ordered water in the X-ray crystal structures.

Finally, as a third possibility, slow exchange not only of the His-117 but also of the His-46 $N^{\epsilon 2}H$ proton might be connected with the fact that the pK_as of His-46 and -117 are affected by their binding to the Cu ion. His-46 and -117 are not titratable between pH 4 and 12. The pK_as for deprotonation of His-46 and -117 could be as large as 13, and the pK_as for protonation of His-46 and -117 could be as low as 3 or less. It can be shown (Englander & Kallenbach, 1984) that under these circumstances base- and acid-catalyzed $N^{\epsilon 2}H$ exchange might be slowed down sufficiently to render the $N^{\epsilon 2}H$ protons observable. Experiments to investigate this question further are in progress.

ACKNOWLEDGMENT

We thank Drs. A. Bax and L. E. Kay for providing us with programs for the processing of 3D spectra. We also wish to thank Mr. J. J. Joordens, Drs. C. Erkelens, and colleagues for technical assistance. Drs. A. Kalverda and colleagues are thanked for helpful discussions. NMR spectra were recorded at the Dutch National Hf-NMR Facility (Nijmegen, The Netherlands), which is supported by the Dutch foundation for Chemical Research (SON).

REFERENCES

Adman, E. T. (1985) *Top. Mol. Struct. Biol. 6*, 1–42.
Adman, E. T. (1991) *Adv. Protein Chem. 42*, 145–197.
Adman, E. T., Canters, G. W., Hill, H. A. O., & Kitchen, N. A. (1982) *FEBS Lett. 143*, 287–292.
Ainscough, E. W., Bingham, A. G., Brodie, A. M., Ellis, W. R., Gray, H. B., Loehr, T. M., Plowman, J. E., Norris, G. E., & Baker, E. N. (1987) *Biochemistry 26*, 71–82.
Baker, E. N. (1988) *J. Mol. Biol. 203*, 1071–1095.
Baker, E. N., Anderson, B. F., Blackwell, K. E., Kingston, R. L., Norris, G. E., & Shepard, W. E. B. (1991) *J. Inorg. Biochem. 43*, 162.
Bax, A. (1989) *Methods Enzymol. 176*, 151–168.
Bax, A., & Davis, D. G. (1985) *J. Magn. Reson. 65*, 355–360.
Bax, A., Griffey, R. H., & Hawkins, B. L. (1983) *J. Magn. Reson. 55*, 301–315.
Bax, A., Ikura, M., Kay, L. E., Torchia, D. A., & Tschudin, R. (1990) *J. Magn. Reson. 86*, 304–318.
Blair, D. F., Campbell, G. W., Schoonover, J. R., Chan, S. I., Gray, H. B., Malmström, B. G., Pecht, I., Swanson, B. I., Woodruff, W. H., Cho, W. K., English, A. M., Fry, H. A., Lum, V., & Norton, K. A. (1985) *J. Am. Chem. Soc. 107*, 5755–5766.
Blaszak, J. A., Ulrich, E. L., Markley, J. L., & McMillin, D. R. (1982) *Biochemistry 21*, 6253–6258.
Braunschweiler, L., & Ernst, R. R. (1983) *J. Magn. Reson. 53*, 521–528.
Brown, S. C., Weber, P. L., & Mueller, L. (1988) *J. Magn. Reson. 77*, 166–169.
Canters, G. W., Hill, H. A. O., Kitchen, N. A., & Adman, E. T. (1984a) *Eur. J. Biochem. 138*, 141–152.
Canters, G. W., Hill, H. A. O., Kitchen, N. A., & Adman, E. T. (1984b) *J. Magn. Reson. 57*, 1–23.
Cavanagh, J., Chazin, W. J., & Rance, M. (1990) *J. Magn. Reson. 87*, 110–131.
Chazin, W. J., & Wright, P. E. (1988) *J. Mol. Biol. 202*, 623–636.
Chazin, W. J., Rance, M., & Wright, P. E. (1988) *J. Mol. Biol. 202*, 603–622.
Clore, G. M., & Gronenborn, A. M. (1991) *Science 252*, 1390–1399.
Driscoll, P. C., Hill, H. A. O., & Redfield, C. (1987) *Eur. J. Biochem. 170*, 279–292.
Driscoll, P. C., Clore, G. M., Marion, D., Wingfield, P. T., & Gronenborn, A. M. (1990) *Biochemistry 29*, 3542–3556.
Englander, S. W., & Kallenbach, N. R. (1984) *Q. Rev. Biophys. 16*, 521–655.
Englander, S. W., & Wand, A. J. (1987) *Biochemistry 26*, 5953–5958.
Fesik, S. W., & Zuiderweg, E. R. P. (1990) *Q. Rev. Biophys. 23*, 97–131.
Goddard, J. M., Caput, D., Williams, S. R., & Martin, D. W. (1983) *Proc. Natl. Acad. Sci. U.S.A. 80*, 4281–4285.
Griesinger, C., Otting, G., Wüthrich, K., & Ernst, R. R. (1988) *J. Am. Chem. Soc. 110*, 7870–7872.
Griesinger, C., Sørensen, D. W., & Ernst, R. R. (1989) *J. Magn. Reson. 84*, 14–63.
Groeneveld, C. M., & Canters, G. W. (1985) *Eur. J. Biochem. 153*, 559–564.
Groeneveld, C. M., & Canters, G. W. (1988) *J. Biol. Chem. 263*, 167–173.
Han, J., Adman, E. T., Beppu, T., Codd, R., Freeman, H. C., Huq, L., Loehr, T. M., & Sanders-Loehr, J. (1991) *Biochemistry 30*, 10904–10913.
Henry, Y., & Bessières, P. (1984) *Biochimie 66*, 259–289.
Hill, H. A. O., & Smith, B. E. (1979) *J. Inorg. Biochem. 11*, 79–93.
Hill, H. A. O., Leer, J. C., Smith, B. E., Storm, C. B., & Ambler, R. P. (1976a) *Biochem. Biophys. Res. Commun. 70*, 331–338.
Hill, H. A. O., Smith, B. E., Storm, C. B., & Ambler, R. P. (1976b) *Biochem. Biophys. Res. Commun. 70*, 783–790.
Kalverda, A. P., Lommen, A., Wijmenga, S., Hilbers, C. W., & Canters, G. W. (1991) *J. Inorg. Biochem. 43*, 171.
Kay, L. E., Marion, D., & Bax, A. (1989) *J. Magn. Reson. 84*, 72–84.
Kumar, A., Ernst, R. R., & Wüthrich, K. (1980) *Biochem. Biophys. Res. Commun. 95*, 1–6.
Light, P. A. P., & Garland, P. B. (1971) *Biochem. J. 124*, 123–134.
Lommen, A., Wijmenga, S., Hilbers, C. W., & Canters, G. W. (1991) *Eur. J. Biochem. 201*, 695–702.
Macura, S., Wüthrich, K., & Ernst, R. R. (1982) *J. Magn. Reson. 46*, 269–282.
Marion, D., & Bax, A. (1988) *J. Magn. Reson. 79*, 352–356.
Marion, D., & Wüthrich, K. (1983) *Biochem. Biophys. Res. Commun. 113*, 967–974.
Marion, D., Kay, L. E., Sparks, S. W., Torchia, D. A., & Bax, A. (1989a) *J. Am. Chem. Soc. 111*, 1515–1517.
Marion, D., Driscoll, P. C., Kay, L. E., Wingfield, P. T., Bax, A., Gronenborn, A. M., & Clore, G. M. (1989b) *Biochemistry 28*, 6150–6156.
Messerle, B. A., Wider, G., Otting, G., Weber, C., & Wüthrich, K. (1989) *J. Magn. Reson. 85*, 608–613.
Mino, Y., Loehr, T. M., Wada, K., Matsubara, H., & Sanders-Loehr, J. (1987) *Biochemistry 26*, 8059–8065.
Moore, J. M., Chazin, W. J., Powis, R., & Wright, P. E. (1988a) *Biochemistry 27*, 7806–7816.
Moore, J. M., Case, D. A., Chazin, W. J., Gippert, G. P., Havel, T. F., Powls, R., & Wright, P. E. (1988b) *Science 240*, 314–317.
Moore, J. M., Lepre, C. A., Gippert, G. P., Chazin, W. J., Case, D. A., & Wright, P. E. (1991) *J. Mol. Biol. 221*, 533–555.
Morris, G. A., & Freeman, R. (1979) *J. Am. Chem. Soc. 101*, 760–762.
Muchmore, D. C., McIntosh, L. P., Russell, C. B., Anderson, D. E., & Dahlquist, F. W. (1989) *Methods Enzymol. 177*, 44–73.
Nar, H., Messerschmidt, A., Huber, R., Van de Kamp, M., & Canters, G. W. (1991a) *J. Mol. Biol. 218*, 427–447.

Nar, H., Messerschmidt, A., Huber, R., Van de Kamp, M., & Canters, G. W. (1991b) *J. Mol. Biol. 221*, 765–772.
Nar, H., Huber, R., Messerschmidt, A., Filippou, A. C., Barth, M., Jaquinod, M., Van de Kamp, M., & Canters, G. W. (1992a) *Eur. J. Biochem. 205*, 1123–1129.
Nar, H., Messerschmidt, A., Huber, R., Van de Kamp, M., & Canters, G. W. (1992b) *FEBS Lett. 306*, 119–124.
Nestor, L., Larrabee, J. A., Woolery, G., Reinhammar, B., Spiro, T. G. (1984) *Biochemistry 23*, 1084–1093.
Oschkinat, H., Cieslar, C., Gronenborn, A. M., & Clore, G. M. (1989) *J. Magn. Reson. 81*, 212–216.
Oschkinat, H., Cieslar, C., & Griesinger, C. (1990) *J. Magn. Reson. 86*, 453–469.
Otting, G., & Wüthrich, K. (1989) *J. Am. Chem. Soc. 111*, 1871–1875.
Otting, G., Liepinsh, E., & Wüthrich, K. (1991a) *J. Am. Chem. Soc. 113*, 4363–4364.
Otting, G., Liepinsh, E., Farmer, B. T., II, & Wüthrich, K. (1991b) *J. Biomol. NMR 1*, 209–215.
Otting, G., Liepinsh, E., & Wüthrich, K. (1991c) *Science 254*, 974–980.
Parr, S. R., Barber, D., Greenwood, C., Phillips, B. W., & Melling, J. (1976) *Biochem. J. 157*, 423–430.
Rance, M., Sørensen, O. W., Bodenhausen, G., Wagner, G., Ernst, R. R., & Wüthrich, K. (1983) *Biochem. Biophys. Res. Commun. 117*, 479–485.
Richardson, J. (1981) *Adv. Protein Chem. 34*, 167–339.
Sambrook, J., Fritsch, E. F., & Maniatis, T. (1989) *Molecular Cloning. A Laboratory Manual*, 2nd ed., Cold Spring Harbor Laboratory Press, Cold Spring Harbor, NY.
Shaka, A. J., Barker, P. B., & Freeman, R. (1985) *J. Magn. Reson. 64*, 547–552.
Shepard, W. E. B., Anderson, B. F., Lewandowski, D. A., Norris, G. E., & Baker, E. N. (1991) *J. Am. Chem. Soc. 112*, 7817–7819.
States, D. J., Haberkorn, R. A., & Ruben, D. J. (1982) *J. Magn. Reson. 48*, 286–292.
Sykes, A. G. (1991) *Adv. Inorg. Chem. 36*, 377–408.
Ugurbil, K., & Bersohn, R. (1977) *Biochemistry 16*, 3016–3023.
Ugurbil, K., & Mitra, S. (1985) *Proc. Natl. Acad. Sci. U.S.A. 82*, 2039–2043.
Ugurbil, K., Norton, R. S., Allerhand, A., & Bersohn, R. (1977) *Biochemistry 16*, 886–894.
Van de Kamp, M., Floris, R., Hali, F. C., & Canters, G. W. (1990a) *J. Am. Chem. Soc. 112*, 907–908.
Van de Kamp, M., Silvestrini, M. C., Brunori, M., Van Beeumen, J., Hali, F. C., & Canters, G. W. (1990b) *Eur. J. Biochem. 194*, 109–118.
Van de Kamp, M., Hali, F. C., Rosato, N., Finazzi Agro, A., & Canters, G. W. (1990c) *Biochim. Biophys. Acta 1019*, 283–292.
Van de Ven, F. J. M., Janssen, H. G. J. M., Gräslund, A., & Hilbers, C. W. (1988) *J. Magn. Reson. 79*, 221–235.
Wijmenga, S. S., & Van Mierlo, C. P. M. (1991) *Eur. J. Biochem. 195*, 807–822.
Wilmot, C. M., & Thornton, J. M. (1990) *Protein Eng. 3*, 479–493.
Wüthrich, K. (1986) *NMR of Proteins and Nucleic Acids*, Wiley, New York.

Registry No. Cu, 7440-50-8.